Article

γ-Linolenic acid in maternal milk drives cardiac metabolic maturation

https://doi.org/10.1038/s41586-023-06068-7

Received: 3 January 2022

Accepted: 11 April 2023

Published online: 24 May 2023

Check for updates

Ana Paredes[1], Raquel Justo-Méndez[1], Daniel Jiménez-Blasco[2,3,4], Vanessa Núñez[1], Irene Calero[1], María Villalba-Orero[1,5], Andrea Alegre-Martí[6], Thierry Fischer[7], Ana Gradillas[8], Viviane Aparecida Rodrigues Sant'Anna[8], Felipe Were[9], Zhiqiang Huang[10], Pablo Hernansanz-Agustín[1], Carmen Contreras[1], Fernando Martínez[9,11], Emilio Camafeita[11,12], Jesús Vázquez[11,12], Jesús Ruiz-Cabello[13,14,15,16], Estela Area-Gómez[17,18], Fátima Sánchez-Cabo[9], Eckardt Treuter[10], Juan Pedro Bolaños[2,3,4], Eva Estébanez-Perpiñá[6], Francisco Javier Rupérez[8], Coral Barbas[8], José Antonio Enríquez[1,4] & Mercedes Ricote[1]✉

Birth presents a metabolic challenge to cardiomyocytes as they reshape fuel preference from glucose to fatty acids for postnatal energy production[1,2]. This adaptation is triggered in part by post-partum environmental changes[3], but the molecules orchestrating cardiomyocyte maturation remain unknown. Here we show that this transition is coordinated by maternally supplied γ-linolenic acid (GLA), an 18:3 omega-6 fatty acid enriched in the maternal milk. GLA binds and activates retinoid X receptors[4] (RXRs), ligand-regulated transcription factors that are expressed in cardiomyocytes from embryonic stages. Multifaceted genome-wide analysis revealed that the lack of RXR in embryonic cardiomyocytes caused an aberrant chromatin landscape that prevented the induction of an RXR-dependent gene expression signature controlling mitochondrial fatty acid homeostasis. The ensuing defective metabolic transition featured blunted mitochondrial lipid-derived energy production and enhanced glucose consumption, leading to perinatal cardiac dysfunction and death. Finally, GLA supplementation induced RXR-dependent expression of the mitochondrial fatty acid homeostasis signature in cardiomyocytes, both in vitro and in vivo. Thus, our study identifies the GLA–RXR axis as a key transcriptional regulatory mechanism underlying the maternal control of perinatal cardiac metabolism.

The mammalian heart requires a continuous supply of energy to maintain cardiac contraction. The highly flexible metabolism of cardiomyocytes enables them to meet their ATP needs by consuming a broad spectrum of substrates including glucose, lipids, lactate, amino acids and ketone bodies, depending on physiological context and age[5]. Fetal cardiomyocytes rely primarily on glucose and lactate oxidation, but the main ATP source after birth is mitochondrial lipid oxidation[1,2,5,6]. However, although the importance of mitochondria in the adult heart is well-established, their contribution to fetal and perinatal heart function has been less explored. The cardiac fetal-to-neonatal switch is believed to occur progressively during the first two weeks of life, culminating in a functional mitochondrial compartment in which fatty acids are efficiently oxidized by β-oxidation[7] (FAO). This adaptive step is crucial for the maintenance of heartbeat and survival, yet very little is known about the molecular mechanisms and upstream signals that instruct this metabolic transition.

RXRs are a nuclear receptor subfamily of ligand-regulated transcription factors that specifically respond to 9-*cis*-retinoic acid and various endogenous fatty acids[8]. Because RXRs operate as both permissive homo- and heterodimers, their ability to be activated by dietary compounds defines them as molecular master sensors that transduce external cues into transcriptional programmes[4]. RXR subtypes are encoded by three genes (in mouse they are *Rxra* (also known as *Nr2b1*), *Rxrb* (*Nr2b2*) and *Rxrg* (*Nr2b3*)), which exhibit time-specific and tissue-dependent differential expression. Whole-body knockout mice lacking RXRα show impaired myocardial growth and die between embryonic day (E)13.5 and E16.5[9,10]. However, specific RXRα depletion in ventricular cardiomyocytes does not result in cardiac

[1]Cardiovascular Regeneration Program, Centro Nacional de Investigaciones Cardiovasculares (CNIC), Madrid, Spain. [2]Institute of Functional Biology and Genomics (IBFG), University of Salamanca, CSIC, Salamanca, Spain. [3]Institute for Biomedical Research of Salamanca (IBSAL), Salamanca, Spain. [4]CIBER de Fragilidad y Envejecimiento Saludable (CIBERFES), Madrid, Spain. [5]Departamento de Medicina y Cirugía Animal, Universidad Complutense de Madrid (UCM), Madrid, Spain. [6]Department of Biochemistry and Molecular Biomedicine, Institute of Biomedicine (IBUB) of the University of Barcelona (UB), Barcelona, Spain. [7]Department of Immunology and Oncology, Centro Nacional de Biotecnología-Consejo Superior de Investigaciones Científicas (CNB/CSIC), Campus Universidad Autónoma de Madrid (UAM), Madrid, Spain. [8]Centro de Metabolómica y Bioanálisis (CEMBIO), Facultad de Farmacia, Universidad San Pablo-CEU, CEU Universities, Madrid, Spain. [9]Bioinformatics Unit, Centro Nacional de Investigaciones Cardiovasculares (CNIC), Madrid, Spain. [10]Department of Biosciences and Nutrition, Karolinska Institutet, Huddinge, Sweden. [11]CIBER de Enfermedades Cardiovasculares (CIBERCV), Madrid, Spain. [12]Proteomics Unit, Centro Nacional de Investigaciones Cardiovasculares (CNIC), Madrid, Spain. [13]CIC biomaGUNE, Basque Research and Technology Alliance (BRTA), San Sebastian, Spain. [14]Ikerbasque, Basque Foundation for Science, Bilbao, Spain. [15]CIBER de Enfermedades Respiratorias (CIBERES), Madrid, Spain. [16]Departamento de Ciencias Farmacéuticas, Facultad de Farmacia, Universidad Complutense Madrid (UCM), Madrid, Spain. [17]Departament of Cellular and Molecular Biology, Centro de Investigaciones Biológicas Margarita Salas-CSIC, Madrid, Spain. [18]Department of Neurology, Columbia University Medical Campus, New York, NY, USA. ✉e-mail: mricote@cnic.es

morphological defects, thus excluding a cell-autonomous role of RXRα expressed in cardiomyocytes[11]. We and others have reported that RXR subtypes show redundancy in several contexts[9,12,13]; however, previous studies have not addressed RXR redundancy in the heart, and the physiological role of RXRs in cardiomyocyte homeostasis remains unknown.

RXR deletion causes lethal cardiac dysfunction

Analysis of RXR subtypes in embryonic and adult hearts revealed progressive increases in *Rxra* and *Rxrb* expression from developmental stages to adulthood, whereas *Rxrg* expression was restricted to postnatal cardiomyocytes (Extended Data Fig. 1a). To dissect RXR function in cardiomyocytes during development, we generated an RXR loss-of-function mouse model by crossing *Nkx2.5-cre* mice, in which the embryonic myocardium is specifically targeted[14], with *Rxra* and *Rxrb* floxed mice[12] ($Rxra^{f/f}Rxrb^{f/f}$). This approach enabled us to avoid compensatory effects between RXR subtypes during cardiac development.

Rxra and *Rxrb* were efficiently deleted in the hearts of embryonic double-knockout ($Nkx2.5\text{-}cre^{+/-}Rxra^{f/f}Rxrb^{f/f}$ (hereafter EDKO)) mice from E11.5 onwards (Extended Data Fig. 1b). Although EDKO newborns were born at Mendelian frequency (data not shown), 80% of EDKO pups died during the first 24 h of life, and no EDKO newborn survived beyond day 7 after birth (Fig. 1a). Extensive echocardiography assessment revealed that EDKO mice progressively underwent severe contractile dysfunction, as shown by gradually decreased ejection fraction (LVEF) within the first 24 h (Fig. 1b, Extended Data Fig. 1c and Supplementary Videos 1 and 2). This change was accompanied by pathological alterations in stroke volume, cardiac output and left ventricle end systolic volume over time. Despite these alterations, the left ventricle diastolic dimension did not change, presumably owing to the rapid onset of death (Extended Data Fig. 1c). The cardiac impairment preceded morbidity of the newborns, suggesting that these heart abnormalities probably contributed to neonatal death. In line with this, EDKO hearts also showed increased expression of the cardiac stress markers *Anf* and *Bnp* (Fig. 1c). These results demonstrate that RXRs expressed in cardiomyocytes exert a cell-autonomous function in the myocardium.

Histological analysis of EDKO hearts revealed no morphological myocardial abnormalities preceeding the cardiac malfunction (Extended Data Fig. 1d–f). Myocardial thickness and the ratio of non-compacted to compacted myocardium were normal (Extended Data Fig. 1d). EDKO pups were slightly smaller than controls but showed no evidence of cardiac hypertrophy or differences in cardiac diameter (Extended Data Fig. 1f,g).

Electrocardiogram (ECG) analysis of postnatal day (P)0 newborns revealed typical ECG traces, with no differences from controls in QRS complex duration or PR, QTc and P intervals (Extended Data Fig. 1h), thus ruling out a contribution to the functional defects from altered rhythmic patterns. We also ruled out leaky expression of the *Nkx2.5-Cre* driver in the brain, liver, stomach, thymus, diaphragm and spleen (Extended Data Fig. 1i). Although subtle gene deletion was observed in the tongue, as previously reported[15], EDKO mice displayed visible milk spots but to a lesser extent than in control pups (Extended Data Fig. 1j), probably owing to a competing disadvantage against wild-type littermates. Further analysis excluded functional irregularities of the lungs (Extended Data Fig. 1k–m) or alternative systemic alterations such as thermogenesis (Extended Data Fig. 1n). These data thus reveal the existence of a physiological mechanism through which RXRs expressed in cardiomyocytes sustain cardiac function and neonatal survival.

RXR drives the switch to neonatal metabolism

Gene expression profiling of P0 hearts (Fig. 1d–f) identified 145 significantly upregulated genes (adjusted P value ≤ 0.05, fold change ≥ 1.5) and 192 significantly downregulated genes (adjusted P value ≤ 0.05, fold change ≤ −1.5) in the EDKO model. Gene ontology analysis highlighted strong downregulation of essential lipid homeostasis-related processes, such as FAO, cholesterol biosynthesis and the L-carnitine mitochondrial shuttle (Fig. 1d). Dysregulated lipid metabolism was further evidenced by transcriptional dampening of the fatty acid homeostasis signature in EDKO hearts (Fig. 1e). Notably, 26.05% of the downregulated genes (50 out of 192) encode mitochondrial proteins related to lipid-derived energy production (Fig. 1f). We called this gene subset the mitochondrial fatty acid homeostasis (mtFAH) cluster. Quantitative PCR with reverse transcription (RT–qPCR) analysis of the mtFAH gene expression signature at gestational and perinatal stages revealed a sharp induction of mtFAH genes from E18.5 to P0 in control hearts. By contrast, mtFAH cluster expression was curtailed in EDKO mice at P0, coinciding with the time of death (Fig. 1g). Prominent cardiomyocyte-intrinsic RXR-controlled genes detected in this analysis included those encoding critical components of lipid droplet homeostasis (*Plin5*), fatty acid activation (*Acsl1* and *Acot1*), fatty acid import to the mitochondrial matrix (*Cpt1a*, *Cpt1b*, *Cpt2* and *Slc25a20*), β-oxidation (*Acadvl*, *Hadha* and *Hadhb*), glucose and fatty acid catabolism balance (*Pdk4* and *Fbp2*), lipid-derived energy dissipation (*Ucp3*), ketogenesis (*Hmgcs2*) and lipogenesis (*Scd4* and *Dgat2*) (Extended Data Fig. 2a). This finding challenges the view that cardiomyocytes acquire the capacity for ATP generation from mitochondrial FAO progressively over the first 15 days of life[5], suggesting instead that cardiomyocytes require mitochondria equipped with the FAO machinery immediately after birth.

To investigate the mechanisms through which transcriptional dysregulation in the EDKO heart might lead to defective lipid-derived energy generation in perinatal cardiomyocytes, we measured ATP production by cardiac P0 mitochondria fed with pyruvate, glutamate, succinate or palmitate (Fig. 2a). No significant differences in ATP production were detected between the genotypes when the substrate was pyruvate, glutamate or succinate, indicating that entry to the electron transport chain by NADH (pyruvate and glutamate) and $FADH_2$ (succinate) was not significantly altered in EDKO mitochondria. By contrast, ATP generation by β-oxidation from palmitate was significantly reduced in EDKO mitochondria. EDKO hearts also showed a significantly decreased rate of palmitate oxidation (Fig. 2b) and decreased fatty acid mitochondrial respiration (Fig. 2c), overall indicating impaired fatty acid import or use. In agreement with these results, an unbiased lipidomics approach highlighted that the depletion of RXRs resulted in significantly lower levels of typical metabolites of FAO such as long-chain acyl-carnitines[16,17] (C14 to C18), and fatty acid esters of hydroxy fatty acids (FAHFAs) (Fig. 2d and Supplementary Table 1). Proteomics analysis of EDKO hearts further confirmed that RXR deletion reduced the abundance of proteins involved in lipid handling (Fig. 2e). Moreover, the hearts of EDKO mice showed altered expression of several proteins related to mitochondrial dynamics and homeostatic pathways, such as reactive oxygen species production, the degradome and the mitochondrial unfolded protein response (Extended Data Fig. 2b). These findings suggest that cardiomyocyte-specific RXR deletion blunts cardiac mitochondrial remodelling towards lipid consumption and synthesis.

This effect was not linked to any alterations to the morphology (Extended Data Fig. 2c,d) or number (Extended Data Fig. 2e) of EDKO mitochondria. Defective lipid-derived ATP production in the absence of RXR suggested that EDKO hearts might commit their metabolism towards anaerobic glucose use. Significantly increased activity of glycolytic flux and lactate production was confirmed by ex vivo quantification (Fig. 2f,g). In parallel, EDKO mice displayed hypoglycaemia and hyperlactaemia (Fig. 2h,i), supporting the idea that RXRs are needed to initiate the fetal-to-neonatal transition. Hence, in their absence, cardiomyocytes remain metabolically immature and unable to establish bioenergetic fitness.

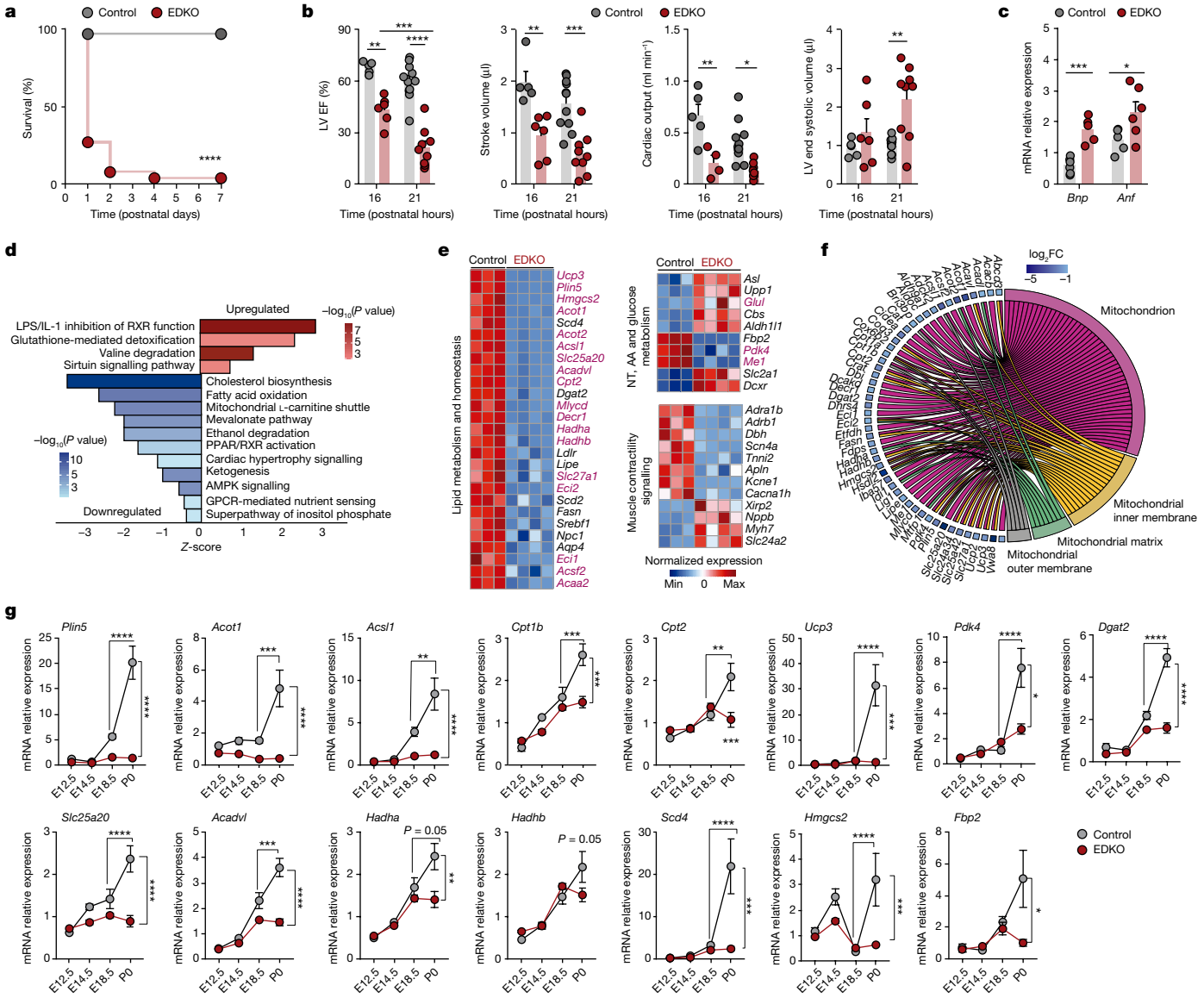

Fig. 1 | EDKO mice undergo lethal cardiac dysfunction and transcriptional alteration of lipid metabolism. a, Kaplan–Meier curves for EDKO and control mice ($n = 27–32$ mice per genotype). Log-rank test ($P < 0.0001$). **b**, Echocardiographic acquisition of EDKO ($n = 6–9$ mice per time point) and control ($n = 5–11$ mice per stage) mice (16 h and 21 h after birth). LVEF, stroke volume, cardiac output and left ventricle (LV) end-systolic volume are shown. Data are mean ± s.e.m. Two-way ANOVA with Tukey post-test. **c**, RT–qPCR quantification of *Bnp* and *Anf* genes in P0 EDKO ($n = 5–6$ mice) and control ($n = 5–6$ mice) hearts. Independent biological replicates. Data are mean ± s.e.m. Two-tailed Student's *t*-test. **d**, Ingenuity pathway analysis biological processes that are changed in P0 EDKO hearts. GPCR, G-protein-coupled receptor; LPS, lipopolysaccharide. **e**, Heat map of normalized RNA-seq expression data for the top differentially expressed genes (DEGs) ($n = 3–4$ mice per genotype, independent biological replicates). Genes are clustered according to biological processes, with genes encoding mitochondrial proteins shaded red. AA, amino acid; NT, nucleotide. **f**, Chord diagram representing cellular component analysis of downregulated mitochondrial protein-encoding genes in EDKO P0 hearts. Shading of squares adjacent to gene symbols indicates the $\log_2$fold change (FC) for EDKO versus control. **g**, Relative quantification by RT–qPCR of FAO gene expression in developmental (E12.5, E14.5 and E18.5) and perinatal (P0) stages of hearts from EDKO ($n = 3–6$) and control ($n = 4–6$) mice. Data are mean ± s.e.m. Two-way ANOVA. Independent biological replicates. $^*P < 0.05$, $^{**}P < 0.01$, $^{***}P < 0.001$, $^{****}P < 0.0001$; NS, not significant. Exact *P* values are provided in Source Data.

Metabolomics profiling of the metabolic status of EDKO hearts using gas chromatography with mass spectrometry revealed a significant decrease in glycerol relative to controls, whereas the amounts of uracil, creatinine and aspartate were increased (Extended Data Fig. 2f). Uracil abundance correlated with the relative mRNA expression of *Upp1*, which encodes the uracil biosynthetic uridine phosphorylase (Extended Data Fig. 2g). The generation of creatinine through the non-enzymatic cyclization of creatine is favoured at low pH[18], and the rise in creatinine could be due to a more acidic cellular environment resulting from the increased lactate production in EDKO hearts. In the case of aspartate, enhanced glucose oxidation is known to promote its biosynthesis in failing cardiomyocytes[19]. Aspartate is also intimately linked to α-ketoglutarate, as both are end-products of glutamate and oxaloacetate transamination[20]. These findings prompted us to explore whether amino acids might contribute to energy homeostasis in EDKO hearts by replenishing Krebs cycle intermediates. Although the amino acid oxidation rate was unaltered (Extended Data Fig. 2h), α-ketoglutarate levels were higher in EDKO hearts (Extended Data Fig. 2i), suggesting that they exhibit imbalanced Krebs cycle activity. These results suggest that RXRs expressed in cardiomyocytes are critical integrators of energy production and mitochondrial maturation immediately after birth.

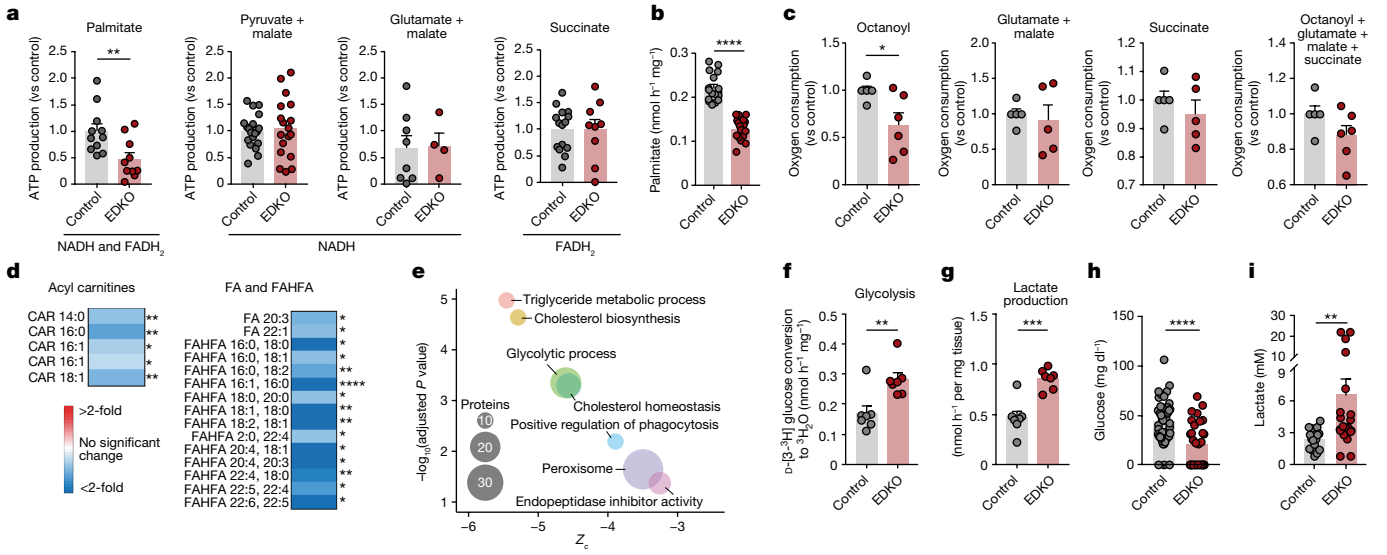

Fig. 2 | Lack of RXR in perinatal cardiomyocytes blocks fetal-to-neonatal metabolic switch. a, Ex vivo ATP production assay in control ($n = 8–19$) and EDKO ($n = 4–18$) P0 cardiac mitochondria supplied with pyruvate (pyruvate + malate), glutamate (glutamate + malate), succinate or palmitate (palmitate + carnitine). In the case of pyruvate or glutamate, malate was added to reach detectable amounts of complex I-dependent ATP synthesis. Individual biological replicates. Data are mean ± s.e.m. Two-tailed Student's *t*-test. Data are normalized as the change versus the change in the control. **b**, Ex vivo β-oxidation flux in control ($n = 17$) and EDKO ($n = 18$) P0 hearts. Individual biological replicates. Data are mean ± s.e.m. Two-tailed Student's *t*-test. **c**, Ex vivo oxygen consumption assay in control ($n = 5$) and EDKO ($n = 5–6$) P0 cardiac mitochondria supplied with octanoyl-carnitine (fatty acid oxidation), glutamate plus malate, succinate and a combination of all substrates. Individual biological replicates. Data are mean ± s.e.m., normalized to the control. Two-tailed Student's *t*-test. **d**, Unbiased lipidomics analysis in control ($n = 4$) and EDKO ($n = 4$) P0 hearts. Acyl-carnitines (CAR), fatty acids (FA) and fatty acid esters of hydroxyl fatty acid (FAHFA) are shown. Data are presented as fold change (EDKO versus control). Independent biological replicates. Two-tailed Student's *t*-test. **e**, Protein function enrichment plot for hearts from P0 EDKO mice ($n = 5$) versus P0 controls ($n = 5$). Independent biological replicates. Dot size indicates the number of proteins in each term. The *x*-axis shows Zc, the standardized variable at the functional category level (EDKO versus control), and the *y*-axis indicates $-\log_{10}$FDRc, the false discovery rate indicating which values stand out as outliers at the functional category level (EDKO versus control). **f**,**g**, Ex vivo glycolytic flux (**f**) and lactate generation (**g**) in control ($n = 7$) and EDKO ($n = 7$) P0 hearts. Independent biological replicates. Data are mean ± s.e.m. Two-tailed Student's *t*-test. **h**, Blood glucose in control ($n = 48$) and EDKO ($n = 30$) (P0) newborn mice. Individual biological replicates. Data are mean ± s.e.m. Mann–Whitney test. **i**, Blood lactate in control ($n = 16$) and EDKO ($n = 20$) (P0) newborn mice. Individual biological replicates. Data are mean ± s.e.m. Mann–Whitney test. $^*P < 0.05$, $^{**}P < 0.01$, $^{***}P < 0.001$, $^{****}P < 0.0001$; NS, not significant. Exact *P* values are provided in Source Data.

RXR remodels cardiac transcription

To determine the molecular basis of the altered metabolic status in P0 EDKO hearts, we conducted a multifaceted genome-wide characterization by assay for transposase-accessible chromatin regions using sequencing[21] (ATAC–seq) and by chromatin immunoprecipitation with sequencing (ChIP–seq) for acytlation of histone 3 lysine 27 (H3K27ac), a histone modification that marks active enhancers and promoters (Fig. 3a). The combination of these techniques allowed us to delineate dynamic changes in chromatin accessibility and activation upon RXR depletion (Fig. 3). ATAC–seq captured 326 differentially open chromatin regions (adjusted *P* value < 0.05, $\log_2$FC > 0.6) and 629 closed regions (adjusted *P* value < 0.05, $\log_2$FC < −0.6) in EDKO versus control P0 hearts, whereas H3K27ac ChIP–seq identified 42 differentially active peaks (adjusted *P* value < 0.05, $\log_2$FC > 0.6) and 650 inactive peaks (adjusted *P* value < 0.05, $\log_2$FC < −0.6) (Fig. 3b and Extended Data Fig. 3a). The relative loss of open and active genomic regions in EDKO hearts suggests that loss of RXRs has an effect on the epigenetic landscape of activated genes in perinatal cardiomyocytes. Moreover, annotation analysis identified similar distributions of ATAC–seq and H3K27ac ChIP–seq differential peaks (Fig. 3c and Extended Data Fig. 3b), with closed and inactive peaks both predominantly annotated as introns (40.22% and 42.62%, respectively) or intergenic regions (36.72% and 31.08%, respectively). This suggests that in perinatal cardiomyocytes, RXRs might have a major role in the distal regulation of chromatin access and transcription via enhancers (Fig. 3c). In line with this idea, transcription factor motif enrichment analysis of these peaks revealed that one of the most frequently found binding motifs was the conventional RXR homodimer response element with 1 nucleotide spacing (DR1), together with motifs for other cardiac-related transcription factors (MEF2 family and GATA4) (Fig. 3d). DR1 motifs are also bound by peroxisome proliferator-activated receptor (PPAR), suggesting that they are plausible heterodimeric partners for cardiac RXRs. Supporting this idea, we found that depletion of RXRs or PPARα result in a similar mtFAH gene expression signature in neonatal hearts (Extended Data Fig. 3c). Notably, the intersection of closed and inactive loci upon RXR depletion demarked the mtFAH signature (Fig. 3e and Extended Data Fig. 3d), indicating that RXRs are specifically required for adaptive epigenetic changes within the regulatory regions of the fatty acid homeostasis gene cluster.

To determine whether the cardiac RXR cistrome included the mtFAH signature, we performed RXR ChIP–seq experiments in control and EDKO neonatal cardiomyocytes. Differential occupancy analysis detected 6,896 loci that contained RXR peaks (10,829 peaks, adjusted *P* value < 0.05, $\log_2$FC > 0.6), defining its cistrome. Transcription factor enrichment analysis revealed the highest enrichment in DR1 and DR4 elements, known motifs for diverse RXR dimers (Extended Data Fig. 3e). Notably, mtFAH signature genes were annotated to the 185 overlapping loci between RXR ChIP–seq, closed ATAC–seq peaks and inactive H3K27ac ChIP–seq peaks (Fig. 3f,g), marking the functional RXR-regulated enhancers and promoters among all RXR-occupied candidate regions (Extended Data Fig. 3f). Furthermore, gene ontology

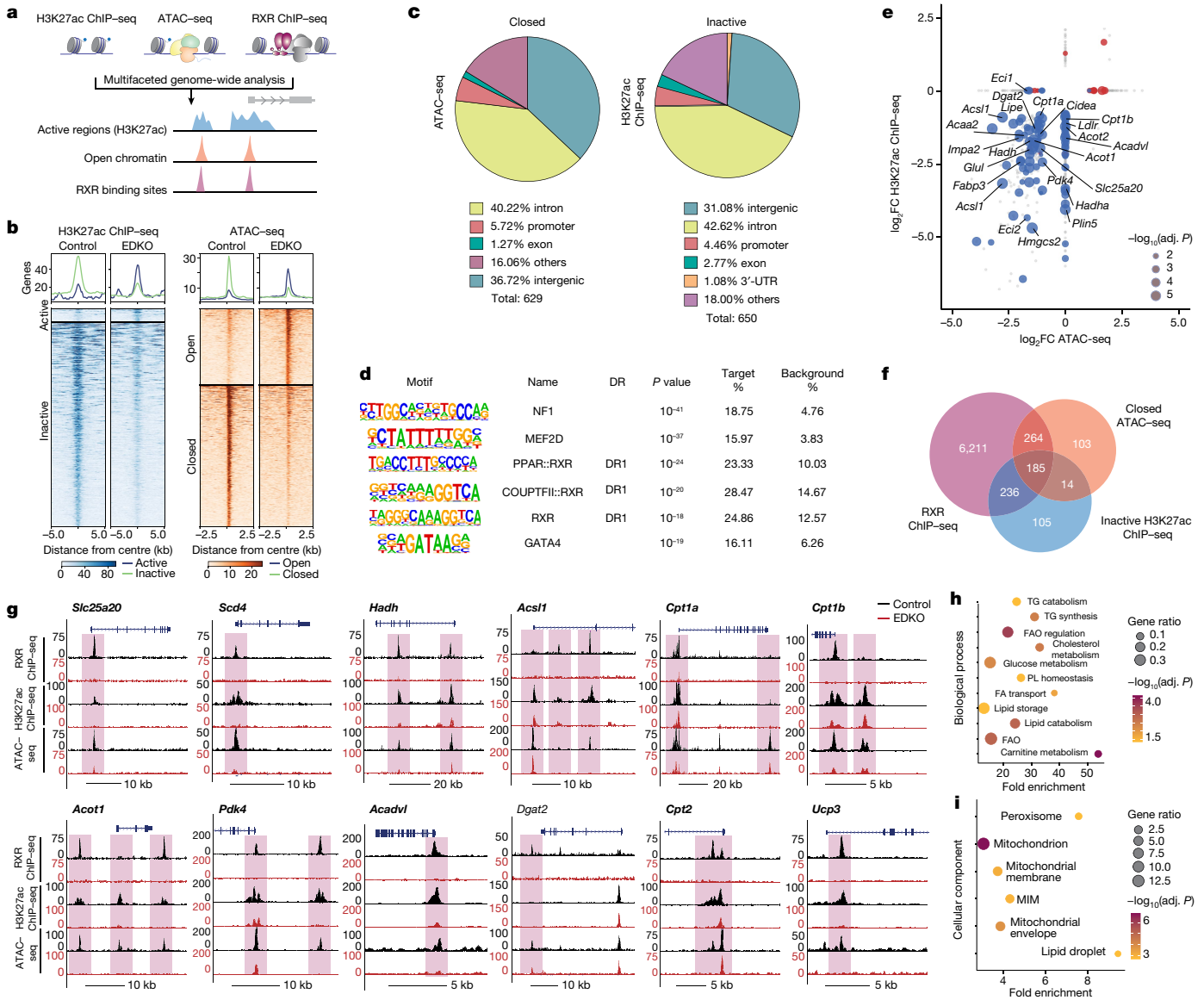

Fig. 3 | RXR transactivates the expression of mtFAH genes. a, Schematic outlining the genome-wide analysis. **b**, Left, H3K27ac ChIP–seq heat map illustrating differentially active or inactive peaks in EDKO hearts. Right, ATAC–seq heat map showing differentially open or closed peaks in EDKO hearts. Adjusted *P* value < 0.05, $\log_2$FC = 0.6; *n* = 2–3 per genotype or experiment, independent biological replicates. Colour bars depict peak intensity. **c**, Annotation distribution of differentially closed peaks (ATAC–seq) and differentially inactive peaks (H3K27ac ChIP–seq) in EDKO P0 hearts. UTR, untranslated region. **d**, HOMER motif enrichment analysis in EDKO P0 hearts. Top-scoring motifs, *P* values, best-match transcription factors, type of nuclear receptor binding DR element, and percentage of target and background sequences are shown. **e**, Intersection of RNA-seq, H3K27ac ChIP–seq and ATAC–seq experiments. For peaks found in only one experiment, a value of 0 was specified for the other axis. Blue and red dots indicate genes significantly downregulated or upregulated according to the $\log_2$FC (RNA-seq). Size indicates $-\log_{10}$(adjusted *P* value) (RNA-seq). Two-tailed Student's *t*-test (Benjamini–Hochberg). For loci absent in the RNA-seq experiment, a size of 1 was specified. **f**, Venn diagram of the RXR cistrome (RXR ChIP–seq), differentially closed annotated loci (closed ATAC–seq), and differentially inactive annotated loci (inactive H3K27ac ChIP–seq) in EDKO hearts. Numbers indicate the number of loci that contained annotated peaks in each experiment. The overlapping section (185 loci) contains the mtFAH signature. **g**, mtFAH loci UCSC tracks identified in the RXR ChIP–seq (*n* = 2 hearts per genotype, independent biological replicates), H3K27ac ChIP–seq and ATAC–seq experiments. Black, control; red, EDKO. Genes encoding mitochondrial proteins are in bold. **h**,**i**, Gene Ontology (GO) enrichment of the 185 annotated mtFAH loci for biological process (**h**) and cellular component (**i**) analysis. Two-tailed Student's *t*-test with Benjamini–Hochberg post-test. MIM, mitochondrial inner membrane; PL, phospholipids; TG, triglycerides.

analysis of the overlapping RXR loci identified lipid homeostasis-related pathways as the most significantly enriched biological process (Fig. 3h) and mitochondria-related compartments as the most enriched cellular compartment (Fig. 3i). We therefore conclude that RXRs operate directly at enhancers and promoters to activate the transcription of mtFAH signature genes and control the surrounding epigenetic landscape in perinatal cardiomyocytes.

Milk fatty acids drive cardiac RXR functions

To confirm that RXR activity directly controls the mtFAH signature and other lipid metabolism-related genes, we administered the selective RXR agonist bexarotene to eight-week-old mice (C57Bl6/J)[12]. RT–qPCR analysis of cardiac tissue from these mice showed that bexarotene significantly induced expression of the mtFAH signature and other

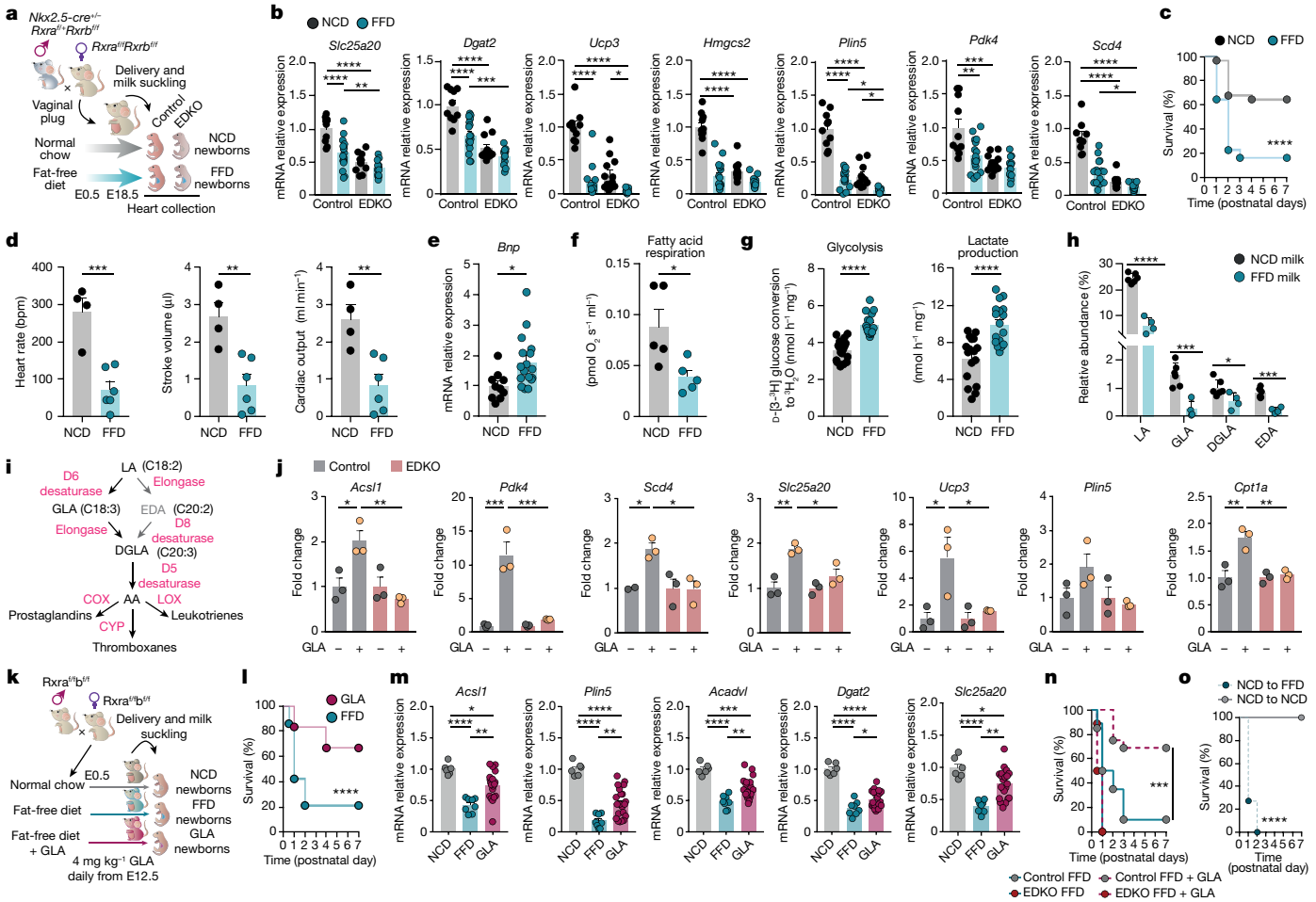

Fig. 4 | Maternal milk-borne GLA activates the RXR-dependent gene signature. a, Experimental outline. **b**, Cardiac expression of mtFAH signature from control ($n = 10–17$) and EDKO ($n = 11–14$) mice (P0) suckled with milk from dams fed a NCD or FFD. Data are mean ± s.e.m. Two-way ANOVA with Tukey's corrections. **c**, Kaplan–Meier curve of control mice fed NCD ($n = 58$) or FFD ($n = 33$) milk. Log-rank test ($P < 0.0001$). **d**, Echocardiography analysis from control newborns (P1) suckling NCD ($n = 4$) or FFD ($n = 6$) milk. Data are mean ± s.e.m. Two-tailed Student's *t*-test. **e**, Cardiac *Bnp* expression in newborn (P1) mice fed NCD (n = 10) or FFD (n = 17) milk. Data are mean ± s.e.m. Two-tailed Student's *t*-test. **f**, β-oxidation oxygen consumption assay in cardiac mitochondria from P1 mice fed NCD ($n = 5$) or FFD ($n = 5$) milk. Data are mean ± s.e.m. Two-tailed Student's *t*-test. **g**, Glycolytic flux and lactate generation in hearts of P1 mice fed NCD ($n = 17$) or FFD ($n = 17$) milk. Data are mean ± s.e.m. Two-tailed Student's *t*-test. **h**, Relative abundance of omega-6 fatty acids in NCD ($n = 6$) and FFD ($n = 4$) milk. LA, linoleic acid; GLA, γ-linolenic acid; DGLA, dihomo-γ-linolenic acid; EDA, eicosadienoic acid. Data are mean ± s.e.m. Two-tailed Student's *t*-test. **i**, The omega-6 fatty acid biosynthesis pathway. AA, arachidonic acid. COX, cyclooxigenase. LOX, lypoxigenase. CYP, CYP450. **j**, In vitro mtFAH gene signature expression in control or EDKO cardiomyocytes treated with GLA–bovine serum albumin (BSA) (500 µM). Data are mean ± s.e.m. ($n = 3$ replicates per condition). Two-way ANOVA. **k**, Outline for rescue of the FFD milk-fed neonatal phenotype. **l**, Kaplan–Meier curve of control mice fed FFD milk (FFD, $n = 64$) or FFD + GLA milk (GLA, $n = 18$). Log-rank test ($P = 0.0003$). **m**, Cardiac mtFAH gene expression in perinatal mice fed NCD milk ($n = 6$), FFD milk (n = 8) or FFD + GLA milk (GLA, $n = 21$) mice. Data are mean ± s.e.m. One-way ANOVA Tukey and Benjamini–Hochberg correction. **n**, Kaplan–Meier curve of control and EDKO mice fed FFD or FFD + GLA milk. Log-rank test ($n = 8–20$ mice per condition), $P = 0.0002$. **o**, Kaplan–Meier curve of control newborns born from NCD-fed mothers but exposed to NCD or FFD milk. Log-rank test, $P < 0.0001$ ($n = 15–22$ mice per group). Independent biological samples in **b**–**h**,**l**–**o**. $^*P < 0.05$, $^{**}P < 0.01$, $^{***}P < 0.001$, $^{****}P < 0.0001$. Exact *P* values in Source Data.

lipid-metabolism genes (Extended Data Fig. 4a), validating the use of this synthetic ligand to modulate RXR-dependent transcriptional circuits in myocardial cells.

The identity of endogenous RXR ligands is a long-standing question, given the central role of RXRs in controlling metabolic homeostasis across the lifespan[22]. In newborns, maternal milk is a powerful source of signalling molecules that can trigger metabolic adaptions by increasing blood lipid content[3,7]. To investigate the effect of lactation on the RXR-dependent mtFAH signature, we analysed relative mRNA expression in control and EDKO hearts from maternal milk-fed or fasted P0 newborns (Extended Data Fig. 4b). *Rxra* and *Rxrb* transcripts were unaltered in milk-fed and fasted control hearts, indicating that maternal milk does not influence RXR abundance (Extended Data Fig. 4c). However, the expression of mtFAH genes (*Slc25a20*, *Ucp3*, *Hmgcs2*, *Plin5* and *Pdk4*) and other lipid homeostasis genes (*Dgat2* and *Scd4*) was significantly reduced in fasted control mice, resembling the EDKO transcriptional phenotype (Extended Data Fig. 4d). Maternal milk deprivation had no effect on lipid homeostasis gene expression in EDKO hearts, suggesting that RXRs are important receptors for milk-derived inducers of the mtFAH transcriptional programme.

Maternal milk is highly enriched in vitamin A and lipids[23,24], the metabolic precursors of RXR ligands[25]. Moreover, nutritional intervention in pregnant mice efficiently modulates maternal milk composition[26]. We therefore investigated whether a lack of fatty acids or vitamin A compounds in milk would prevent RXR-dependent mtFAH transcriptional induction in offspring (Fig. 4a and Extended Data Fig. 4e–g). For these

experiments, we crossed *Nkx2.5-cre*$^{+/-}$*Rxra*$^{f/+}$*Rxrb*$^{f/f}$ male mice with *Rxra*$^{f/f}$ *Rxrb*$^{f/f}$ females, and fed *Rxra*$^{f/f}$*Rxrb*$^{f/f}$ dams with a normal chow diet (NCD), a fat-free diet (FFD) or a vitamin A-deficient (VAD) diet from E0.5 onwards. Lactation was monitored, and control and EDKO hearts were collected from pups 4 h after birth (Fig. 4a). Hearts from neonates fed milk from dams on the VAD (VAD milk) had a normal mtFAH gene expression profile, indicating that 9-*cis*-retinoic acid is not the relevant RXR ligand in perinatal cardiomyocytes (Extended Data Fig. 4e). By contrast, hearts from pups fed milk from dams on a FFD (FFD milk) showed a pronounced reduction in the expression of mtFAH signature genes and other lipid metabolism-related genes (Fig. 4b), matching the effect observed in milk-deprived neonates (Extended Data Fig. 4d). Other key metabolic genes involved in glycolysis, Krebs cycle or mitochondrial oxidative phosphorylation complexes were not changed in hearts from pup fed FFD milk (Extended Data Fig. 4f). The residual mtFAH signature in EDKO hearts was largely insensitive to the FFD milk, with only mild decreases in *Ucp3* and *Plin5* gene expression (Fig. 4b). Because expression of *Rxra* and *Rxrb* was insensitive to FFD milk (Extended Data Fig. 4g), these data support the conclusion that RXRs expressed in cardiomyocytes relay signals from maternal milk-derived fatty acids (milk-FA) to enable mitochondrial maturation and metabolic adaptation in neonatal hearts.

To determine whether a lack of milk-FA reproduces the RXR-deficient phenotype, we examined control newborns suckled with either milk from dams fed a NCD (NCD milk) or FFD milk upon delivery. Whereas neonates fed NCD milk thrived, control mice fed FFD milk died within 48 h of birth (Fig. 4c) and showed a significant reduction in body weight at P1 (Extended Data Fig. 4h). Echocardiography analysis showed that feeding on FFD milk severely impaired cardiac function in the pups (Fig. 4d, Extended Data Fig. 4i and Supplementary Videos 3 and 4). Cardiac defects in control pups fed FFD milk included significantly decreased heart rate, stroke volume, cardiac output and LVEF compared to pups fed NCD milk (Fig. 4d and Supplementary Videos 3 and 4). Moreover, the hearts of pups fed FFD milk showed reduced LV telediastolic volume (Extended Data Fig. 4i). Consistent with these findings, neonates fed FFD milk exhibited significantly increased cardiac expression of *Bnp* mRNA (Fig. 4e). We excluded other causes of death for the pups fed FFD milk, such as thermogenesis or lung oedema (Extended Data Fig. 4j,k). In addition, control hearts from pups fed FFD milk showed reduced fatty acid mitochondrial respiration and enhanced glycolysis and lactate production (Fig. 4f,g). Together, these results indicate that milk-FA support metabolic adaptation in the neonatal heart and suggest that activation of a milk-FA–RXR axis is a relevant mechanism for sustaining perinatal life.

GLA–RXR drives mitochondrial maturation

We next aimed to identify the endogenous RXR ligand in maternal milk. To precisely dissect the contribution of each milk-FA, we performed an unbiased lipidomics analysis comparing the milk-FA profiles in NCD milk and FFD milk (Supplementary Table 2). Milk-FAs that were significantly diminished in milk from dams fed the FFD would be candidate RXR ligands. We detected 45 free fatty acids and estimated their abundance as the relative proportion within their fatty acid class: saturated (SAFA), monounsaturated (MUFA), di-unsaturated (DUFA) and polyunsaturated (PUFA) fatty acids. The family of omega-6 fatty acids exhibited the most significant decrease in FFD milk compared with NCD milk (P value < 0.05, $\log_2$FC < 0, mean content in NCD milk > 0.5%). Specifically, LA (C18:2n-6), GLA (C18:3n-6), DGLA (C20:3n-6) and EDA (C20:2n-6) (Fig. 4h and Extended Data Fig. 4l,m). Omega-6 fatty acids are a family of important bioactive PUFAs that is generated through an elongation cascade from LA, an essential fatty acid that is provided only by dietary intake and therefore cannot be compensated by endogenous maternal synthesis[27] (Fig. 4i). The presence of LA, GLA, DGLA and EDA has been widely reported in human breast milk, which provides the required physiological source of omega-6 fatty acids to the human newborn[27–30].

LA and GLA bind the ligand-binding domain of RXRα and stabilize RXRα heterodimerization, respectively[31,32]. To assess whether these omega-6 fatty acids induce the mtFAH signature, we analysed gene expression in C57B6/J primary neonatal cardiomyocytes and the HL-1 cardiac muscle cell line treated with LA or GLA (Extended Data Fig. 5a–d). The synthetic RXR agonist LG268[12] was used as an additional pharmacological approach and served as a control. GLA and LG268 both strongly increased mtFAH gene expression, whereas LA had no effect (Extended Data Fig. 5a–d). We further demonstrated that GLA-induced mtFAH gene expression is RXR-dependent, as the GLA effect was lost in EDKO primary cardiomyocytes (Fig. 4j) as well as in C57B6/J primary neonatal cardiomyocytes pretreated with UVI3003 (UVI), an RXR antagonist[33] (Extended Data Fig. 5e). We further determined the absolute concentration of GLA (from all lipid forms) in cardiac tissue (30.4 μmol kg^{-1}) as well as in NCD milk (1,066.3 ± 167.4 μM) and FFD milk (335.9 μM ± 165.4 μM), showing a substantial decrease in FFD milk compared with NCD.

Additionally, to validate the physiological role of GLA derived from maternal milk in metabolic cardiac maturation, we aimed to rescue the FFD phenotype by selectively restoring GLA levels in FFD milk (Fig. 4k). Neonates that were fed milk from dams on a FFD supplemented with GLA (FFD + GLA milk) thrived and had normal body weight, glycaemia and ability to feed compared to neonates fed FFD milk (Fig. 4l and Extended Data Fig. 5f–h). Moreover, mtFAH gene expression in perinatal hearts of mice fed FFD + GLA milk was significantly increased (Fig. 4m and Extended Data Fig. 5i), suggesting that GLA is a critical signal to ensure neonatal cardiac transcriptional energetics. Rescue of survival in neonates fed FFD + GLA milk was RXR-dependent, supporting the existence of a GLA–RXR transcriptional axis in perinatal cardiomyocytes (Fig. 4n). In alternative approaches, customized FFD diets supplemented with LA and GLA or GLA alone rescued lethality in neonates fed FFD milk (Extended Data Fig. 5j). Notably, pups delivered by NCD mothers and exposed to FFD milk died, supporting the role of maternal milk, and not lipid deposits during pregnancy, as the relevant GLA source for ensuring perinatal survival (Fig. 4o).

To provide more direct evidence that GLA binds to RXR, we first confirmed the interaction of GLA with recombinant RXRα ligand-binding domain (RXRα-LBD) in vitro using surface plasmon resonance (Fig. 5a), showing that unliganded RXRα-LBD bound GLA with a dissociation constant (K_d) of 10.9 ± 7.1 μM. Moreover, GLA binding to the RXRα-LBD induced the recruitment of a steroid receptor coactivator-derived LxxLL peptide with a K_d of 80.9 ± 3.6 μM (Fig. 5b,c). This result indicates that in the presence of RXR ligand, the AF2 coactivator-binding surface had acquired the active conformation capable of recruiting coactivators[34]. We further used a GAL4-UAS-driven luciferase reporter to monitor the activity of the wild-type RXRα-LBD fused to a GAL4 DNA-binding domain (RXRα-LBD–GAL4-DBD) or RXRα-LBD(ΔAF2)–GAL4-DBD, which lacks the AF2 helix 12 that is required for ligand-dependent transcriptional activation[9,35], in the presence of GLA (Fig. 5d). GLA treatment significantly induced luciferase activity in cells expressing RXRα-LBD–GAL4-DBD but not in cells expressing RXRα-LBD(ΔAF2)–GAL4-DBD (Fig. 5d). Notably, blockade of RXRα–GAL4 binding by the RXR antagonist UVI3003 abolished the GLA-mediated luciferase induction (Fig. 5d). In addition, we corroborated the ability of GLA to stabilize the RXRα–SRC1 coactivator complex in a ligand-dependent manner (Fig. 5e). These assays were reproduced in an alternative system where RXRα or RXRα-ΔAF2 plasmids were cotransfected with a reporter plasmid containing three copies of the $(AOX)_3$ response element (RXR response element-specific binding sites) (Extended Data Fig. 5k–m). Finally, in silico modelling revealed structural docking of GLA in the RXRα ligand-binding pocket, generating a stable GLA–RXRα complex (Fig. 5f and Supplementary Table 3). Overall, these data demonstrate that GLA is a potential ligand for RXR.

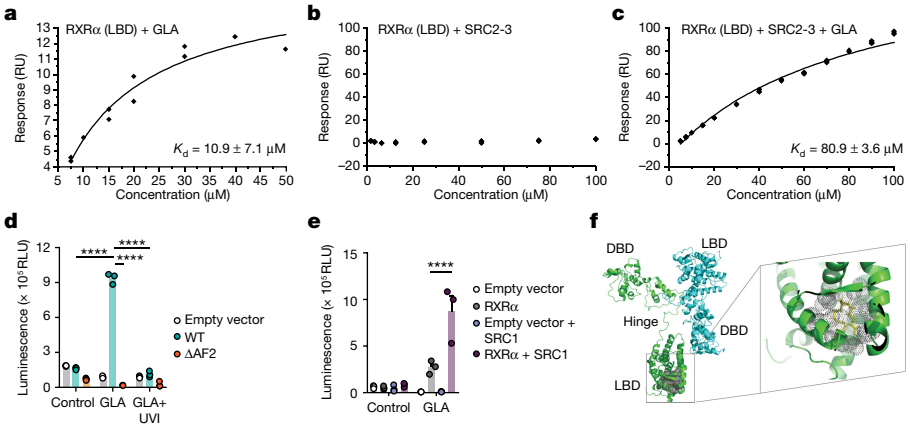

Fig. 5 | GLA is a potential ligand for RXR. a–**c**, Surface plasmon resonance analysis of the interaction of unliganded RXRα-LBD with increasing concentrations of GLA (**a**), SRC2-3 coactivator (**b**) or SRC2-3 coactivator in the presence of a saturating concentration of 120 μM GLA (**c**). The results of experiments conducted in duplicate are shown along with the calculated K_d. The maximum binding signal (R_{max}) and chi-squared calculated from the 1:1 Langmuir fitting were 19.82 resonance units (RU) and 0.510 RU^2 (**a**) and 30.00 RU and 1.66 RU^2 (**c**), respectively. **d**, Representative experiment (out of three) with the GAL4-UAS-driven luciferase reporter assay in HEK293T cells. Cells were transfected with empty vector (control), wild-type RXRα-LBD–GAL4-DBD (WT) or mutated RXRα-LBD(ΔAF2)–GAL4-DBD (ΔAF2) for 6 h (n = 3 technical replicates per condition). Then, cells were treated with 500 μM GLA–BSA (GLA) or 500 μM GLA–BSA with 1 μM UVI3003 (UVI) for 24 h. Data are mean ± s.e.m. Two-way ANOVA with Tukey post-test. RLU, relative light units. **e**, Representative experiment (out of 3) of GAL4-UAS-driven luciferase reporter assay to monitor ligand-dependent coactivator recruitment in HEK293T cells. Transient transfections were performed with a limiting amount of wild-type RXRα-LBD–GAL4-DBD and/or SRC1 coactivator for 6 h. Then, cells were treated with 500 μM GLA–BSA for 24 h (n = 3 technical replicates per condition). Data are mean ± s.e.m. Two-way ANOVA with Tukey post-test. **f**, In silico model of GLA docking in the ligand-binding domain of the mouse RXRα dimer. Left, 3D view (cartoon representation) illustrating RXRα chain A in green and chain B in cyan. The ligand cavity is represented as grey dots. Right, zoomed view of GLA docking in the ligand cavity of chain A. The ligand cavity is represented as grey dots and GLA as a yellow stick model. ****P < 0.0001. Exact P values are provided in Source Data.

Discussion

The neonatal cardiac dysfunction and death of mice lacking cardiomyocyte RXRα and RXRβ demonstrates that myocardial-specific RXRs have a cell-autonomous role in cardiac physiology. Furthermore, given the absence of cardiac abnormalities in ventricle-restricted RXRα-deficient mice[11] and the full RXRβ-deficient mice[36], our results show that RXR subtypes can compensate for each other's absence in myocardial cells. In agreement with previous reports[37,38], we have excluded myocardial RXRs as transcriptional controllers of cardiac morphogenesis. In this setting, the structural abnormalities observed in the myocardium of full RXRα-deficient mice[10] may be owing to the loss of epicardial-specific RXRα action, which has been proposed to regulate cardiomyocyte growth via WNT signalling in a paracrine fashion[39].

Although our study identifies RXRs as the key transcription factors controlling the fetal-to-neonatal metabolic transition, the extent to which this activity relies on RXR homodimers or heterodimers with other nuclear receptors is currently difficult to estimate. Transcription factor motif analysis indicates that the DR1 motif is enriched at RXR target gene loci, including the mtFAH signature. Of note, the DR1 motif is recognized by both RXR homodimers and heterodimers with PPARs, which are expressed in embryonic cardiomyocytes. Indeed, we show that PPARα-deficient neonatal hearts also display a downregulated mtFAH gene signature. However, unlike RXRs, PPARα is not essential in the heart, since PPARα-knockout mice have a milder phenotype that does not compromise neonatal survival[40]. This could be a consequence of functional redundancy among the PPAR subtypes [9,12,13]. Alternatively, the cooperation of RXR with other transcription factors or nuclear receptors could contribute to the lethality in EDKO mice. Along with the EDKO phenotype, the induction of the mtFAH signature by the endogenous ligand GLA and the RXR-selective agonist LG268 strongly supports the active role of RXRs, irrespective of the distinct RXR dimer states.

Our results identify the essential omega-6 PUFA GLA as a critical maternal milk nutrient for proper cardiac adaptation and survival in newborn mice, demonstrating that GLA is a potential RXR ligand in perinatal cardiomyocytes. The obligate dietary intake of GLA could establish a checkpoint in newborns, as only dams that are not nutritionally deprived will be able to provide their progeny with GLA and thus support proper nutritional health and growth. We also found that non-essential fatty acids were dispensable for cardiac mitochondrial maturation, in line with a report that offspring survival is unaffected by conditional deletion of the key lipogenic enzyme PERK[41]. The death of EDKO neonates makes it difficult to dissect the functional implications of GLA–RXR signalling on postnatal cardiac physiology. An intriguing question for future research is whether the GLA–RXR axis has a conserved role in the perinatal adaptation of other organs.

A technical limitation of our study was the inability to specifically quantify the absolute amount of GLA in the FFD + GLA milk, and therefore we cannot exclude the possibility of other metabolites being involved in this context. Moreover, the potential relevance of our findings for human physiology should be investigated further. Carnitine-acylcarnitine translocase deficiency (CACTD) is a life-threatening metabolic disease that provokes heart failure and neonatal death in humans. CACTD is caused by mutations in the RXR-controlled gene *SLC25A20*[42]. Therefore, it would be interesting to explore whether modulation of RXR transcriptional pathways would be an effective therapeutic approach for CACTD. From a nutritional standpoint, low GLA abundance in human maternal milk has been linked to growth deficits in newborns[43], suggesting a potential role of this fatty acid in human neonatal physiology. Our results reinforce the emerging idea that mother–infant interactions in early life are major drivers of organismal physiology and highlight the importance of maternal milk ingestion for mitochondrial maturation of perinatal hearts, a finding with major implications for cardiac health.

Online content

Any methods, additional references, Nature Portfolio reporting summaries, source data, extended data, supplementary information, acknowledgements, peer review information; details of author contributions and competing interests; and statements of data and code availability are available at https://doi.org/10.1038/s41586-023-06068-7.